S - 7

Quality Control for SPECT Instrumentation

Hiroyuki Shinohara, Tomoaki Yamamoto, Yoshio Kuniyasu, Munehiro Takahashi[1] and Takashi Yokoi[1]

Dept. of Radiology, Showa University Fujigaoka Hospital
[1] Dept. of Medical Systems, Shimadzu Corporation

1. INTRODUCTION

The purpose of routine quality control (QC) of scintillation camera-based SPECT system is to detect changes in performance from a base line condition. The base line characterization is made by acceptance testing. We measured intrinsic uniformity and spatial linearity of scintillation cameras with field uniformity correction devices in combination with the performance tests developed by national electrical manufacturers association (NEMA standard)[1]. Using this results we understood the base line condition of scintillation cameras and continued weekly QC test of intrinsic spatial linearity for 26 weeks and of intrinsic uniformity for five years.

We used SPECT system equipped with simultaneous transmission and emission data acquisition protocol (PRISM 3000, Ohio Imaging of Picker International). Custom phantoms were used to evaluate the accuracy of linear attenuation coefficient measured with transmission computed tomography (TCT), and to evaluate combined scatter and attenuation correction in ^{201}Tl SPECT imaging.

2. METHOD

2-1. QC for scintillation camera

1) Intrinsic flood field uniformity was measured as "integral uniformity" (a maximum deviation) and a "differential uniformity" (a maximum rate of change over a specified distance, roughly slope) for the useful field-of-view (UFOV) of the camera (the collimated field-of-view), and central field-of-view (CFOV) of the camera (the 75% of the linear dimensions of the UFOV).

$$Integral\ uniformity = \pm\ 100\ \frac{(Max - Min)}{(Max + Min)}, \quad (1)$$

$$Differential\ uniformity = \pm\ 100 \left(\frac{Largest\ slice\ deviation\ (Hi - Low)}{Hi + Low} \right), \quad (2)$$

where differential uniformity was determined for maximum change of count density over a range of 5 pixels in all rows and columns.

2) Intrinsic spatial resolution was measured in both the X and Y directions and expressed as full width half maximum (FWHM) and full width tenth maximum (FWTM) of the line spread function measured in millimeters for slit phantom in Fig. 1 (intrinsic spatial resolution test pattern). Black dots (●) in Fig.1 denote the peak location of line spread function determined every 30 mm in Y direction using Gaussian fitting algorithm with weighted least squares.

3) Intrinsic spatial differential linearity and absolute spatial linearity in both X and Y directions were measured using slit phantom 1. Differential linearity (expressed in millimeters) is the standard deviation of line spread function peak separations in the CFOV and UFOV. Absolute linearity was measured from the same slit phantom data and was expressed as the maximum amount of spatial displacement measured.

Fig. 1

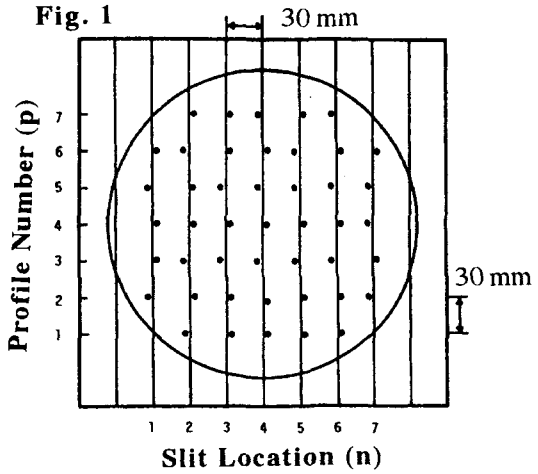

Fig. 2(a)

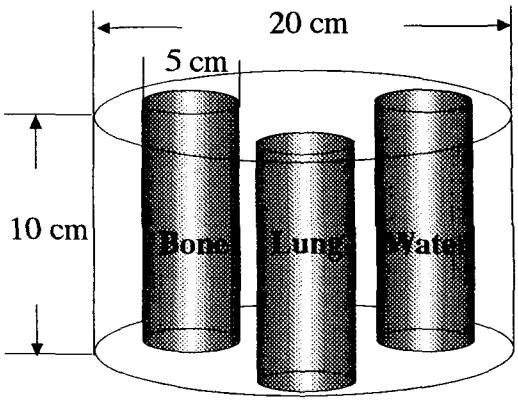

The peak location of line spread function, $l_{n,p}$, corresponding to each slit number, n, is searched in the profile, p, every 30-mm step from the center of slit phantom image. In order to find a set of lines that are equally spaced and parallel but are allowed to have a slight angle with the coordinate axis, following multiple regression is used:

$$L_{n,p} = B_1 + B_2 n + B_3 p, \tag{3}$$

where B_1, B_2, and B_3 are fitting constants to be determined. Maximum distance between the fitted parallel lines, $L_{n,p}$, and real data for each peak locations, $l_{n,p}$, is the absolute linearity calculated as:

$$\left|\Delta_{n,p}\right|_{\max} = maximum \left| L_{n,p} - l_{n,p} \right|. \tag{4}$$

In place of differential linearity the mean distance, $\bar{\Delta}$, is used in the present work.

$$\bar{\Delta} = \frac{1}{N}\sum_{i=1}^{N} \left| L_{n,p} - l_{n,p} \right|, \tag{5}$$

where N is the total peak locations measured in the CFOV or UFOV.

4) Multiple window spatial registration is a parameter of cameras which characterizes positional deviation in the image at different energies. If the spatial registration of photons with three different energies (93 keV, 185 keV and 300 keV) of ^{67}Ga was not precisely aligned, the spatial resolution with ^{67}Ga three-window imaging was lower than that of single-window imaging using 93-keV photon alone[2].

2-2. QC for SPECT

The accuracy of linear attenuation coefficients measured with TCT in simultaneous transmission (^{99m}Tc) and emission (^{201}Tl) data acquisition was examined with phantom composed of three kinds of tissue-equivalent absorbers simulating the attenuation of lung, water and compact bone for 140-keV photon energy and have linear attenuation coefficients of 0.045 cm^{-1}, 0.151 cm^{-1} and 0.269 cm^{-1} respectively (Fig. 2(a)). If outer cylinder was filled with water alone and transmission scan was performed, we measures the linear attenuation coefficient without crosstalk from the high energy photopeaks of ^{201}Tl (135 keV and 167 kev). This simulates that transmission

and emission data are acquired separately (sequential data acquisition mode). If it was filled with solution of ^{201}Tl and transmission and emission data were simultaneously acquired, we measures the linear attenuation coefficient in the presence of crosstalk from the high energy photopeaks of ^{201}Tl.

Reconstruction accuracy for line source in the presence of attenuating medium was evaluated using line source embedded in concentrically piled up acrylic disks (concentric disk phantom; Fig. 2(b)). Projections underwent different magnitude of scatter and attenuation dependent on the diameter of disk. If both scatter and attenuation were accurately compensated, total counts, peak counts and FWTM of reconstructed line spread function should be constant along the phantom depth defined by the distance to one of six disks from the disk with 6 cm diameter.

Quantitative accuracy of radioactivity concentration was measured using a cylinder with 5.5 cm in diameter and 10 cm in height containing 179 kBq ml^{-1} solution of ^{201}Tl (hot-rod insert) positioned 2.5 cm from the center of cylinder with 20 cm in diameter and 10 cm in height filled with 44.7 kBq ml^{-1} solution of ^{201}Tl as a background activity (Fig. 2(c)). Reconstructions were performed with ordered subset expectation maximization algorithm (OSEM).

Fig. 2(b)

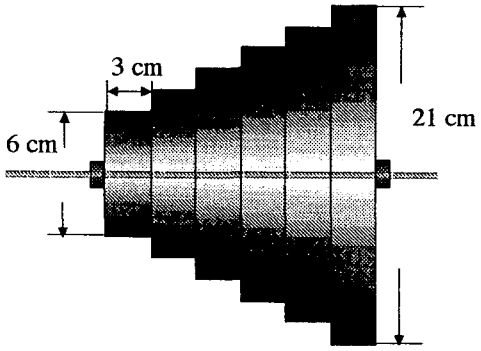

Fig. 2(c)

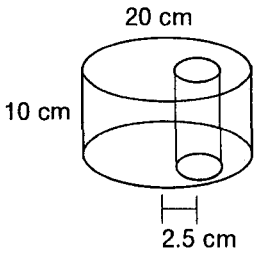

Fig. 2(d)

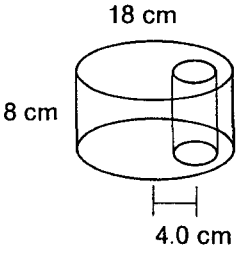

3. RESULTS

3-1. QC for scintillation camera

Figure 3 shows the integral uniformity monitored for five years based on weekly QC program[3].

Fig. 3

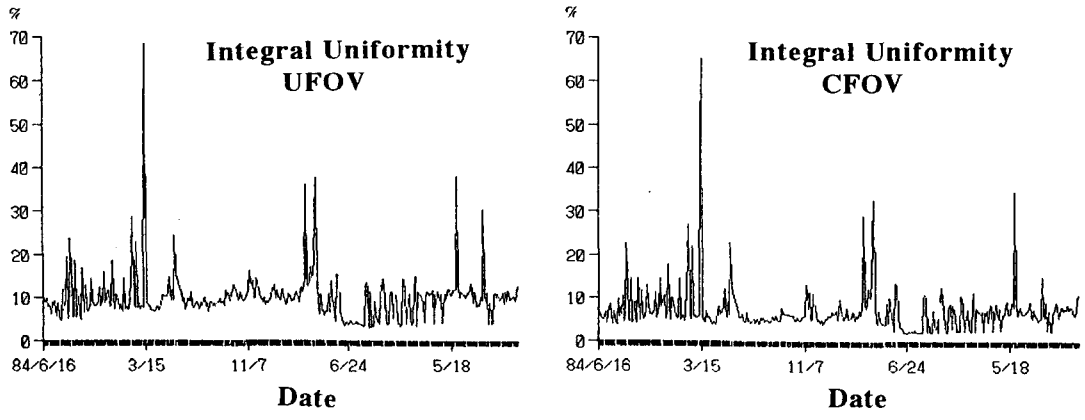

3-2. QC for SPECT

The measured linear attenuation coefficients by TCT for 140-keV photons were shown in Table 1. Figure 4 shows the total counts and FWTM measured for concentric disk phantom. The total counts, peak counts, and FWTM were roughly constant along the phantom depth if both scatter and attenuation correction was performed (AC+ SC+) (AC+: with attenuation correction; AC-: without attenuation correction; SC+: with scatter correction; SC-: without scatter correction). Mean relative error in radioactivity concentration for 10 ROIs including hot-rod and background areas for phantom in Fig. 2(c) was 6.0% and image contrast 3.86:1 (true 4:1).

Table 1. Accuracy of linear attenuation coefficient (cm^{-1}) evaluated by tissue-equivalent phantom.

	Lung	Water	Bone
Calculated	0.045	0.151	0.269
Sequential[1)]	0.064	0.140	0.253
Simultaneous[2)]	0.062	0.139	0.242

1) Phatom is filled with water alone, 2) Phantom is filled with ^{201}Tl solution.

Fig. 4

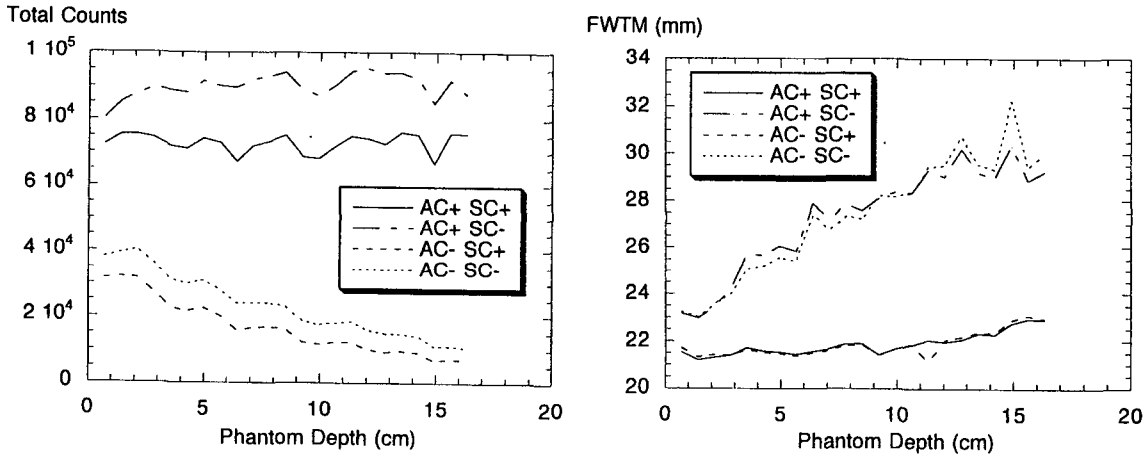

4. DISCUSSION

Photon attenuation and scatter in cardiac SPECT are major factors contributing to quantitative inaccuracy and the decrease in contrast of defect lesions. Therefore it is advisable to include test for scatter and attenuation correction into SPECT performance test as well as uniformity, statistical noise and spatial resolution of reconstructed image.

References

1) Standards Publ. No. NU1-196. Performance measurements of scintillation cameras. National Electrical Manufactures Association (1994)

2) Shinohara H and Koga Y: Ga-67 imaging with scintillation camera: The selection of collimator. J. Nucl. Med. **22**: 169-176, 1981

3) Shinohara H, Hasebe S, Uchiyama K, et al.: Quality control of SPECT on the basis of analytical SPECT reconstruction methods. Jpn. J. Med. Phys. **17**: 18-36,1997

4) Matsuoka S, Shinohara H, Yamamoto T, et al.: Combined scatter anf attenuation correction for Tl-201 myocardial perfusion SPECT using OSEM algorithm. J. Nucl. Med. **40**: 299, 1999 (Abstract)